The Proteasome Inhibitor Bortezomib Induces Apoptosis in Human Retinoblastoma Cell Lines In Vitro

Vassiliki Poulaki,[1] *Constantine S. Mitsiades,*[2] *Vassiliki Kotoula,*[3] *Joseph Negri,*[2] *Douglas McMillin,*[2] *Joan W. Miller,*[1] *and Nicholas Mitsiades*[2]

Purpose. To evaluate the potential of proteasome inhibitors, a novel class of antitumor agents, for the treatment of retinoblastoma. The proteasome inhibitor bortezomib (PS-341, Velcade; Millennium Pharmaceuticals, Cambridge, MA), approved by the US Food and Drug Administration for the treatment of multiple myeloma, is being studied for the treatment of several other malignancies. Among other effects, it inactivates the transcription factor nuclear factor-κB (NF-κB) by blocking the degradation of its inhibitor, IκB. NF-κB, which is constitutively active in human retinoblastoma cells and promotes their survival, represents a therapeutic target for patients with this malignancy.

Methods. The authors evaluated the effect of bortezomib on the retinoblastoma cell lines Y79 and WERI-Rb1 in vitro using a 3-(4,5-dimethylthiazol-2-yl)-2,5-diphenyltetrazolium bromide (MTT) assay, flow cytometry with propidium iodide, gene expression profiling, RT-PCR, and immunoblotting.

Results. Bortezomib induced caspase-dependent apoptosis in both retinoblastoma cell lines at clinically achievable concentrations. Bortezomib upregulated heat-shock proteins, other stress-response proteins, proapoptotic molecules, cell-cycle regulators, transcription factors, cytokines, and several proteasome subunits and solute carrier proteins, whereas it downregulated antiapoptotic and adhesion molecules. Bortezomib also induced cleavage of caspases, Bid and poly(ADP-ribose) polymerase (PARP), and sensitized retinoblastoma cells to doxorubicin.

Conclusions. Bortezomib induces a stress response and triggers caspase-dependent apoptosis in human retinoblastoma cells at clinically achievable concentrations. This study provides insight into the molecular mechanism(s) of the antitumor activity of bortezomib and a basis for future preclinical studies leading to clinical trials of bortezomib, alone or in combination with conventional chemotherapy, to improve patient outcomes in retinoblastoma. (*Invest Ophthalmol Vis Sci.* 2007;48:4706–4719) DOI:10.1167/iovs.06-1147

From the [1]Angiogenesis/Laser Laboratory, Department of Ophthalmology, Massachusetts Eye and Ear Infirmary, Harvard Medical School, Boston, Massachusetts; the [2]Department of Medical Oncology, Dana Farber Cancer Institute, and Department of Medicine, Harvard Medical School, Boston, Massachusetts; and the [3]Department of Pathology, School of Medicine, Aristotle University of Thessaloniki, Thessaloniki, Greece.

Supported by the Knights Templar Eye Foundation.

Submitted for publication September 24, 2006; revised March 26 and June 5, 2007; accepted July 31, 2007.

Disclosure: **V. Poulaki**, None; **C.S. Mitsiades**, Millennium Pharmaceuticals (C, R); **V. Kotoula**, None; **J. Negri**, None; **D. McMillin**, None; **J.W. Miller**, None; **N. Mitsiades**, None

The publication costs of this article were defrayed in part by page charge payment. This article must therefore be marked "*advertisement*" in accordance with 18 U.S.C. §1734 solely to indicate this fact.

Corresponding author: Vassiliki Poulaki, Angiogenesis/Laser Laboratory, Department of Ophthalmology, Massachusetts Eye and Ear Infirmary, Harvard Medical School, 243 Charles Street, Boston, MA 02114; poulakiv@hotmail.com.

The 26S proteasome is a large adenosine triphosphate (ATP)-dependent multimeric complex that degrades intracellular proteins targeted for proteolysis by the process of ubiquitination.[1–4] Protein ubiquitination followed by proteasome-mediated degradation is a major pathway for protein turnover, but it also plays an important role in intracellular signaling through modulation of the levels of intracellular signaling mediators, such as the inhibitor of nuclear factor-κB (NF-κB) IκB,[5] p53,[6–8] and c-Jun N-terminal kinase (JNK).[9] Proteasome inhibitors constitute a novel class of antitumor agents with preclinical evidence of activity against hematologic malignancies and solid tumors.[10,11] Specifically, bortezomib, a boronic acid dipeptide with selective activity as a proteasome inhibitor, has demonstrated clinical efficacy in patients with multiple myeloma[12] and is approved by the US Food and Drug Administration (FDA) for that indication.[13] It is under evaluation for its activity in a variety of other hematologic and solid malignancies.[14–18]

An important effect of proteasome inhibition on cell biology is the abrogation of proteasomal degradation of the NF-κB inhibitor IκB. Proteasome inhibitors induce cytoplasmic accumulation of IκB, which then blocks the nuclear translocation and transcriptional activity of NF-κB. Other NF-κB–independent effects of bortezomib on myeloma cells include the stabilization of p53 protein and the upregulation of p53 mRNA, the stabilization of c-*myc*,[19] and the phosphorylation and activation of c-Jun.[19] These effects may contribute to the proapoptotic impact of bortezomib in various different types of cancer cells in vitro and, possibly, in vivo.[19,20] It appears that cancer cells are more sensitive than healthy cells to proteasome inhibition, possibly because of their chaotic cell cycles and their genetic instability. Moreover, bortezomib sensitizes malignant cells to cytotoxic chemotherapeutic agents by downregulation of the NF-κB–dependent expression of several inhibitors of apoptosis such as A1, cellular inhibitor of apoptosis protein-2 (cIAP2), and X-linked inhibitor of apoptosis protein (XIAP).[21]

Retinoblastoma is the most common intraocular malignancy of childhood. Human retinoblastoma cells exhibit constitutive transcriptional activity of NF-κB, which is necessary for their survival.[22] Therefore, therapeutic strategies targeting NF-κB could be beneficial in the clinical management of retinoblastoma. In this study, we evaluated the in vitro effect of bortezomib on the retinoblastoma cells lines WERI-Rb1 and Y79. We found that both retinoblastoma cell lines were sensitive to bortezomib and underwent caspase-dependent apoptosis. These studies therefore provide the framework for the use of proteasome inhibitor–based therapies in the treatment of aggressive retinoblastomas.

Materials and Methods

Cell Lines

The human retinoblastoma cell lines Y79 and WERI-Rb1 were purchased from the American Type Culture Collection (Manassas, VA) and grown in Dulbecco modified Eagle medium (DMEM; BioWhittaker, Walkersville, MD) with 100 U/mL penicillin, 100 μg/mL streptomycin, and 10% fetal calf serum (FCS; Invitrogen, Carlsbad, CA).

Reagents

Bortezomib (PS-341, Velcade, pyrazylCONH(CHPhe)CONH(CHisobutyl)B$(OH)_2$; Millennium Pharmaceuticals, Cambridge, MA) was dissolved in dimethyl sulfoxide (DMSO) and stored at −20°C until use. Bortezomib was diluted in culture medium immediately before use. Bortezomib and control media contained less than 0.0005% DMSO. The pan-caspase inhibitor benzyloxycarbonyl-Val-Ala-Asp(OMe)-fluoromethylketone (ZVAD-FMK) was purchased from Calbiochem (La Jolla, CA) and was used at 20 μM; 3-(4,5-dimethylthiazol-2-yl)-2,5-diphenyltetrazolium bromide (MTT) and doxorubicin were from Sigma Chemical (St. Louis, MO).

Cell survival was examined using the MTT colorimetric assay[19] and propidium iodide staining,[23] as previously described. Immunoblotting analysis was performed as previously described.[23] Antibodies used were mouse monoclonal antibodies for Bcl-2 (clone C-2), Bax (clone 2D2), and tubulin (clone B-7); polyclonal antibodies for caspases-3 and -9 (Santa Cruz Biotechnology, Santa Cruz, CA); monoclonal antibody for p53 (clone BP53–12) and polyclonal antibodies for inhibitor of caspase-activated DNAse (ICAD)/DNA fragmentation factor (DFF45), phospho-c-Jun and total c-Jun (Upstate Biotechnology, Lake Placid, NY); monoclonal antibody for Noxa (clone 114C307.1; Alexis Biochemicals, San Diego, CA); monoclonal antibody for poly(ADP-ribose) polymerase (PARP) (clone C-2 to C-10; Biomol, Plymouth Meeting, PA); monoclonal antibody for p21 (clone DF10) and Bcl-x_L (clone 2H12; Calbiochem); and polyclonal antiserum against phospho-IκB (Ser32), total IκB, p27, Bid, XIAP, p53-upregulated modulator of apoptosis (PUMA), and caspase-12 (Cell Signaling, Beverly, MA).

Global Gene Expression Profiling of Bortezomib-Treated Cells

Total RNA was extracted and purified with the RNeasy kit (Qiagen, San Diego, CA). Five micrograms of total RNA was used in the first-strand cDNA synthesis with T7-$d(T)_{24}$ primer (GGCCAGTGAATTGTAATACGACTCACTATAGGGAGGCGG-$(dT)_{24}$) and Superscript II (Invitrogen). Second-strand cDNA synthesis was carried out at 16°C by adding *Escherichia coli* DNA ligase, *E. coli* DNA polymerase I, and RNase H to the reaction, followed by T4 DNA polymerase to blunt the ends of newly synthesized cDNA. cDNA was purified through phenol/chloroform and ethanol precipitation. The purified cDNA was incubated at 37°C for 5 hours in an in vitro transcription reaction to produce cRNA labeled with biotin (BioArray High Yield RNA Transcript Labeling Kit; Enzo Diagnostics, Farmingdale, NY).

Affymetrix Chip Hybridization

cRNA (20 μg) was fragmented by incubation in buffer containing 200 mM Tris-acetate (pH 8.1), 500 mM KOAc, and 150 mM MgOAc at 94°C for 35 minutes. The hybridization cocktail containing 15 μg adjusted fragmented cRNA mixed with eukaryotic hybridization controls (control cRNA and oligonucleotide B2) was hybridized with a pre-equilibrated human chip (U133 2.0 Plus; Affymetrix Inc., Santa Clara, CA) at 45°C for 16 hours. After the hybridization cocktails were removed, the chips were washed in a fluidic station with low-stringency buffer (6× standard saline phosphate with EDTA, 0.01% Tween 20, and 0.005% antifoam) for 10 cycles (2 mixes/cyc) and high-stringency buffer (100 mM N-morpholino-ethanesulfonic acid [MES]), 0.1 M NaCl, and 0.01% Tween 20) for four cycles (15 mixes/cyc) and stained with streptavidin phycoerythrin. This process was followed by incubation with normal goat IgG and biotinylated mouse anti-streptavidin antibody and restaining with streptavidin phycoerythrin. The chips were scanned (HP ChipScanner; Affymetrix Inc.) to detect hybridization signals.

Data Analysis

Scanned image output files were visually examined for major chip defects and hybridization artifacts and then were analyzed with microarray analysis software (GeneChip Microarray Analysis Suite 5.0; Affymetrix). The image from each gene chip was scaled such that the average intensity value for all arrays was adjusted to a target intensity of 150. Expression analysis files created by the software were exported as flat text files to a spreadsheet (Excel; Microsoft, Redmond, WA) for further analysis. Data analysis identified signals with at least a twofold difference between bortezomib-treated samples and respective controls. These results were screened for $P < 0.0025$, Student's *t*-test, to identify induced or repressed transcripts. Information and annotations for all genes were retrieved using the NetAffx website (www.affymetrix.com/analysis/index.affx) and UnChip (unchip.org:8080/bio/unchip; Alberto Riva, Atul Butte, and Isaac Kohane; Children's Hospital, Boston), as previously reported,[19] and were added to the data file. Annotated data were sorted according to functional relationships.

Validation of Expression Array Results by RT-PCR

Confirmation of the microarray results was performed for selected genes, chosen based on putative function, by RT-PCR. Primers for 80- to 130-bp PCR targets were designed with primer analysis software (Oligo 6.69; Molecular Biology Insights, Cascade, CO; Table 1). Y79 cells treated with bortezomib for 0, 2, 4, 8, 16, and 24 hours were harvested, and RNA was extracted with reagent (TRIzol-LS; Invitrogen), according to manufacturer's instructions. RNA was further cleaned with an additional DNAse I digestion step using a commercial kit (RNeasy Micro kit; Qiagen), according to manufacturer's instructions. Reverse transcription was performed for equal RNA amounts (1 μg, as measured by UV spectrophotometry) with random hexamers and reagent (Superscript II; Invitrogen) with a final step of RNase H digestion (all reagents from Invitrogen). PCR amplification of the resultant cDNAs was performed with PCR beads (Ready-to-Go; Amersham), with final concentrations of 2 mM for $MgCl_2$ and 150 to 200 nM each primer, for 45 cycles at annealing temperatures, depending on each primer set (60°C-68°C). The housekeeping gene was hypoxanthine guanine phosphoribosyltransferase 1 (*HPRT1*). Protocols were standardized for optimal annealing temperatures, amplification thresholds, and specificity of melting curves with SYBR Green I in a DNA engine (Opticon; MJ Research, Waltham, MA) with the version 2.01 software (Opticon; MJ Research). PCR products were visualized by electrophoresis on 2% agarose gels.

Statistical Analysis

To evaluate the differences across various experimental conditions in the viability experiments with bortezomib, one-way analysis of variance was performed, and post hoc tests (Duncan and Dunnett T3 tests) were used to evaluate differences between individual pairs of experimental conditions. IC_{50} was calculated with the help of statistical analysis software (Statistica; StatSoft, Tulsa, OK). In all analyses, $P < 0.05$ was considered statistically significant.

Results

Effect of the Proteasome Inhibitor Bortezomib on Survival of Retinoblastoma Cells

We treated the retinoblastoma cell lines Y79 and WERI-Rb1 in vitro with bortezomib (0–100 nM) for 24 hours and evaluated their viability using the MTT assay. These cell lines were sensitive to bortezomib-induced cell death and had IC_{50} values of 10 and 4.4 nM, respectively (calculated by MTT; Fig. 1A). Concentrations were well within those achieved clinically in patients treated with bortezomib.[18] Bortezomib-treated cells exhibited a prominent sub-G_1 peak on propidium iodide analysis, indicating induction of apoptosis (Figs. 1B, 1C).

Effect of Bortezomib on the NF-κB Inhibitor IκB

We next investigated the effect of proteasome inhibition on cellular levels of the NF-κB inhibitor IκB levels in retinoblastoma cells. We found that bortezomib treatment resulted in the accumulation of phosphorylated and total IκB levels (Fig. 2).

TABLE 1. RT-PCR Primers for Transcripts Selected for Validation

Gene		Primer Sequence (5′–3′)	Amplicon Length (bp)	Annealing Temperature (°C)
ATF3	F	TGTCCATCACAAAAGCCGAGGTAGC	107	60
	R	CTCCTTCTTCTTGTTTCGGCACT		
ATF5	F	CCCCCTGGCTCCCTATGAGGTCCTT	120	68
	R	GCTGTGAAATCAACTCGCTCAGTCA		
JUN	F	GCCAGAGCCCTGTTGC	102	60
	R	GAAGGTCGTTTCCATCTTTGC		
Noxa	F	GGGAAGAAGGCGCGCAAGAACG	118	68
	R	GTTTCTGCCGGAAGTTCAGTTTGTC		
p21/CIP1/WAF1	F	GTCACTGTCTTGTACCCTTGTG	129	60
	R	CGGCGTTTGGAGTGGTAGAAA		
p27/KIP1	F	AAGCGACCTGCAACCGACGATTCTT	100	60
	R	GCTCCACAGAACCGGCATTT		
GADD45B	F	GGGGTGTACGAGTCGGCCAAGTTGA	106	60
	R	GGATTTGCAGGGCGATGTCA		
GADD45G	F	CGAGTCAGCCAAAGTCTTGAACGTG	121	60
	R	GAAAGCCTGGATCAGCGTAAA		
GADD153	F	TGTCTTCAGATGAAAATGGGGGTAC	95	60
	R	CAGAGAAGCAGGGTCAAGAGT		
HSP70B	F	GTGGGGGCACCTTCGATGTGT	118	60
	R	TGGTTCACGAGCCGGTTGT		
Hsp105	F	CCCCGTCAGTCATATCATTTGG	81	60
	R	TGTTTGCATGAGTGATTTGCTG		
Survivin	F	GCCCAGTGTTTCTTCTGCTTCAAGG	105	60
	R	ACAGAAAGGAAAGCGCAACC		
HPRT1	F	TGGACAGGACTGAACGTCTTG	111	60
	R	CCAGCAGGTCAGCAAAGAATTTA		

F, forward primer; R, reverse primer.

Transcriptional Profile of Bortezomib-Treated Retinoblastoma Cells

To define molecular pathways regulating proteasome inhibitor-induced apoptosis, we characterized the gene expression profiles of Y79 and WERI-Rb1 cells treated with bortezomib (25 nM for 2–24 hours) and compared the profiles with those of vehicle-treated controls harvested at the same time point using the human gene chip (U133 2.0 Plus; Affymetrix). Analyses of these gene expression profiles showed that bortezomib induced distinct patterns of coordinated changes in a range of transcripts, including the downregulation of growth and anti-apoptotic transcripts, the induction of members of proapoptotic and stress cascades, the upregulation of components of the proteasome/ubiquitin pathway, and an especially potent upregulation of heat-shock protein (HSP) transcripts. Lists of known genes whose transcripts demonstrated the most prominent changes on treatment with bortezomib are presented in Tables 2 and 3. For validation, selected transcripts were studied by RT-PCR (Fig. 3).

Effect of Bortezomib Treatment on p53, p21, and p27 Expression

We investigated further the mechanism of bortezomib-induced apoptosis. Subsequent experiments were performed in both retinoblastoma cell lines and yielded similar results (representative results are shown). We evaluated the protein levels of p53, a proteasome substrate,[6–8] p21, and p27 in bortezomib-treated retinoblastoma cells. We found that bortezomib potently increased the protein levels of p53, p21, and p27 (Fig. 4). This pathway may contribute to the antigrowth and proapoptotic effects of bortezomib on retinoblastoma cells.

Effect of Bortezomib Treatment on c-Jun Phosphorylation

Treatment with bortezomib resulted in the upregulation of c-Jun mRNA (Tables 2 and 3), c-Jun protein, and phospho-c-Jun (Fig. 4) levels.

Role of Caspases in Bortezomib-Induced Apoptosis in Retinoblastoma Cells

We then investigated the role of caspases in bortezomib-induced apoptosis of retinoblastoma cells. Bortezomib induced the cleavage of caspases during apoptosis in retinoblastoma cells (Fig. 5A). Cleavage of the caspase substrate PARP was also detected on bortezomib-treated cells, confirming the enzymatic activation of caspases (Fig. 5A). Pretreatment of retinoblastoma cells with the pan-caspase inhibitor ZVAD-FMK (20 μM) starting 1 hour before treatment with bortezomib had a strong attenuating effect on bortezomib-induced apoptosis (Figs. 5B–D). Overall, our data support a role for the caspase cascade as a mediator of bortezomib-induced apoptosis in retinoblastoma cells.

Involvement of Bcl-2 Family Members in Bortezomib-Induced Apoptosis of Retinoblastoma Cells

We then studied the expression of several members of the Bcl-2 family of apoptosis modulators. We detected the cleavage of Bid, which is a proapoptotic member of the family, and the upregulation of Noxa and PUMA, in agreement with our microarray data (Fig. 6A). These data suggest an implication of Bcl-2 family members in bortezomib-induced apoptosis of retinoblastoma cells.

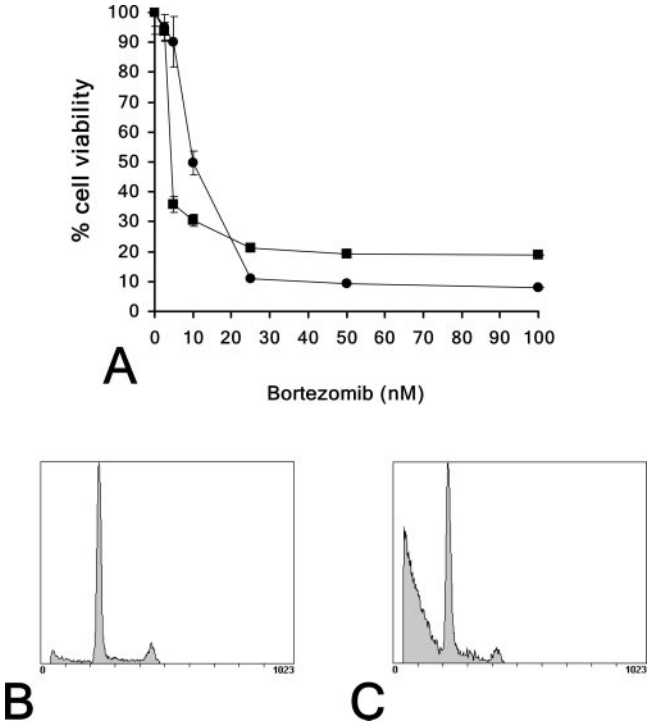

FIGURE 1. Induction of apoptosis in retinoblastoma cells by proteasome inhibition. (**A**) Dose-response curves of retinoblastoma cells treated with bortezomib for 24 hours. WERI-Rb1 (■) and Y79 (●) cells were treated with bortezomib for 24 hours in serum-free medium. Cell survival was quantified using the MTT assay, and values were expressed as percentages over those of vehicle-treated controls. All experiments were repeated at least three times, and each experimental condition was repeated at least in quadruplicate wells in each experiment. Data reported are mean ± SD of representative experiments. (**B**, **C**) The cell cycle profile of bortezomib-treated Y79 cells was evaluated by propidium iodide (PI) analysis and flow cytometry. Y79 cells were treated with bortezomib (25 nM for 24 hours in serum-free medium) or vehicle, and their cell cycle profile was compared with that of control cells (treated with an equal volume of DMSO). Although vehicle-treated cells (**B**) exhibited a standard profile of distribution in the various phases of the cell cycle (G_0/G_1, S, and G_2/M), the cell cycle profile of bortezomib-treated cells (**C**) was hallmarked by the detection of a prominent peak in the sub-G_1 region, suggesting significant bortezomib-induced apoptosis.

Effect of Bortezomib Treatment on Heat Shock Protein Expression

Treatment of retinoblastoma cells with bortezomib resulted in the potent upregulation of HSP70 mRNA (as shown earlier) and protein (Fig. 6B) and the less prominent upregulation of HSP90.

Effect of Bortezomib Treatment on Doxorubicin-Induced Apoptosis in Retinoblastoma Cells

We studied the effect of bortezomib on the response of retinoblastoma cells to the chemotherapeutic drug doxorubicin, which is frequently used for the treatment of retinoblastoma. We found that bortezomib enhanced the proapoptotic effect of doxorubicin (Fig. 7).

DISCUSSION

In the present study, we investigated the impact of the proteasome inhibitor bortezomib on retinoblastoma cell lines and found that it induces caspase-dependent apoptosis at concentrations well below the trough levels of bortezomib observed in pharmacokinetic studies in humans[18] and significantly lower than those necessary to kill cells from solid tumors (colon, ovary, prostate). These findings support the use of proteasome inhibitor-based therapies in the treatment of aggressive retinoblastomas.

Proteasome inhibitors represent a novel class of antineoplastic agents that target several signaling pathways simultaneously: they block the degradation and lead to the accumulation of IκB,[5] which prevents the activation of transcription factor NF-κB[5,19]; they stabilize the proapoptotic p53 protein[6–8]; and they induce the activation of the JNK/jun pathway,[19] reactive oxygen species (ROS) production and resultant mitochondrial injury,[24] and the caspase pathway.[19] Bortezomib, a potent proteasome inhibitor that shows no significant inhibitory activity against other enzymatic systems, has demonstrated clinical activity in patients with relapsed refractory multiple myeloma[12] and has been approved by US FDA for this indication.[13] Phase 1 studies in pediatric patients with refractory solid tumors and hematologic malignancies have demonstrated that bortezomib is well tolerated in children. The recommended phase 2 dose of bortezomib for children with solid tumors is 1.2 mg/m^2 per dose, and for children with leukemia it is 1.3 mg/m^2 per dose, administered as an intravenous bolus twice weekly for 2 weeks followed by a 1-week break.[25,26]

As do multiple myeloma cells, retinoblastoma cells exhibit high baseline NF-κB activity, which is necessary for their survival.[22] In the present study, bortezomib-induced inhibition of IκB degradation by the proteasome resulted in IκB accumulation, which would bind NF-κB and sequester it in the cytoplasm, preventing its translocation to the nucleus and sensitizing the cell to apoptosis. The proteasome inhibitor MG132 has also been shown to stabilize p53 and IκB and to act synergistically with sodium butyrate in inducing apoptosis of Y79 cells.[27]

To better characterize the effects of bortezomib on retinoblastoma cells and to delineate its signaling pathways, we studied the expression profile of bortezomib-treated retinoblastoma cells using microarray analysis. We found that bortezomib treatment results in a specific coordinated pattern of transcriptional events consistent with its proapoptotic effects—the downregulation of transcripts involved in key growth/survival signaling pathways and the upregulation of transcripts implicated in proapoptotic and stress pathways. Other gene families that were modulated were those of the HSP-ubiquitin-proteasome pathway and solute carrier/transport proteins. This transcriptional profile of the bortezomib-treated retinoblastoma cells was remarkably similar between the two retinoblastoma

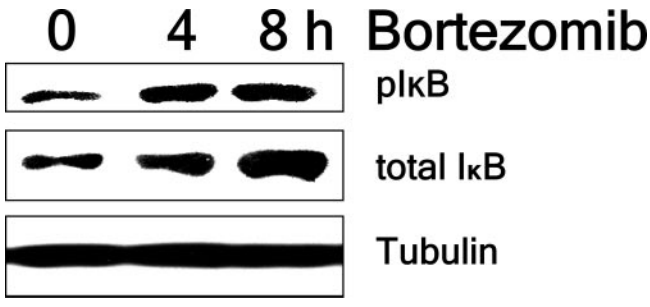

FIGURE 2. Bortezomib treatment of retinoblastoma cells results in accumulation of the NF-κB inhibitor IκB. WERI-Rb1 cells were treated with bortezomib (25 nM) for 0 to 8 hours. Total cell lysates were assayed by immunoblotting for the presence of phosphorylated and total IκB. Tubulin is shown as a loading control. Bortezomib induced the accumulation of phosphorylated and total IκB.

TABLE 2. Transcriptional Profiles of Bortezomib-Treated WERI-Rb1 Cells by Oligonucleotide Microarray Analysis

Gene Name	Accession No.	2 h	4 h	8 h	16 h	24 h
Adhesion						
Intercellular adhesion molecule 2	NM 000873	−1.04	1.35	1.54	2.07	3.05
Cell membrane glycoprotein (adhesion regulating molecule 1 [*ADRM1*])	NM 007002	1.17	1.72	2.9	3.43	2.89
Neural cell adhesion molecule 1	AA126505	1.12	−1.22	−1.47	−3.09	−4.31
Apoptosis						
TSSC3	AF001294	−1.06	1.46	2.66	35.1	36
Clusterin (complement lysis inhibitor, SP-40,40, sulfated glycoprotein 2)	M25915	−1.01	−1.06	11	24.2	21.3
Serine/threonine kinase 17a	AW194730	1.09	1.33	3.43	7.02	5.96
Harakiri, Bcl-2 interacting protein	NM 003806	1.18	1.2	2.42	6.87	4.79
Phosphatidylserine receptor	AK021780	1.15	1.45	1.88	3.64	3.34
Phorbol-12-myristate-13-acetate-induced protein 1 (*NOXA*)	AI857639	−1	1.59	2.03	2.25	2.32
BH3 interacting domain death agonist (*Bid*)	NM 001196	−1.02	1.01	−1.06	−1.28	2.03
Bcl-2 binding component 3 (*PUMA*)	AF332558	1.11	1.22	2.53	3.1	1.01
Baculoviral IAP repeat-containing 5 (survivin)	AA648913	1.04	−1.25	−1.99	−2.44	−2.42
Cell cycle						
S100 calcium binding protein A2	NM 005978	1.14	−1.08	−1.02	4.37	8.08
Pelota homolog	NM 015946	1.3	2.1	2.36	3	3.49
Cyclin-dependent kinase inhibitor 1A (p21, Cip1)	NM 000389	1.11	1.43	2.41	2.41	1.46
Transcription factor Dp-1	NM 007111	−1.14	−1.12	−1.68	−4.65	−4.91
Putative c-Myc responsive	NM 006443	1.09	−1.41	−2.82	−10.6	−9.15
Cytoskeleton						
Neurofilament 3 (150-kDa medium)	NM 005382	1.1	1.41	2.68	5.32	6.91
Vimentin	AI922599	−1.06	1.11	1.13	4.84	6.42
Stathmin-like 4	NM 030795	−1.07	−1.29	1.31	5.38	5.67
Lamin A/C	NM 005572	1.18	1.28	2.01	3.47	2.84
Filamin A, alpha (actin-binding protein 280)	NM 001456	1.13	1.32	2.35	2.19	1.56
Microtubule-associated protein 1A	AW296788	1.21	3.23	3.19	2.51	1.16
Differentiation						
msh homeobox homolog 1	NM 002448	−1.13	−1.04	1.74	9.47	9.5
Doublecortex; lissencephaly, X-linked (doublecortin)	NM 000555	−1.05	−1.28	−2.77	−7.46	−10.1
DNA/RNA metabolism and function						
Splicing factor, arginine/serine-rich 10 (transformer 2 homolog, *Drosophila*)	U87836	−1.24	1.31	2.38	3.95	5.21
BRF2, subunit of RNA polymerase III transcription initiation factor, BRF1-like	AF298153	1.74	3.32	4.41	4.67	4.99
U6 snRNA-associated Sm-like protein	AA112507	−1.07	−1.08	−2.88	−5.63	−3.8
H1 histone family, member 2	BC002649	1.05	−1.21	−4.88	−5.03	−4.53
Endonuclease G	NM 004435	1	−1.31	−3.68	−5.7	−5.34
Polymerase (DNA directed), delta 2, regulatory subunit (50 kDa)	NM 006230	−1.03	−1.11	−1.99	−5.66	−6.09
Extracellular matrix						
Nidogen (enactin)	NM 002508	−1.09	1.2	1.38	5.35	7.27
Collagen, type 1, alpha 1	K01228	1.05	−1.03	1.04	5.6	6.43
Tuftelin 1	NM 020127	1.24	1.02	1.71	4.66	4.5
Collagen, type XVIII, alpha 1	NM 030582	1.04	1.01	1.18	2.1	3.48
Collagen, type III, alpha 1	AU144167	1.56	1.5	1.25	2.62	2.71
Heat shock protein						
Heat shock 70-kDa protein 1A	NM 005345	−1.14	1.14	2.44	50.3	82.5
Heat shock 70-kDa protein 1B	NM 005346	−1.08	−1.03	2.99	54.9	81.8
Heat shock 70-kDa protein 6 (HSP70B′)	NM 002155	1.06	−1.02	26.8	67.9	69.2
Crystallin, alpha B	AF007162	−1.06	−1.02	1.66	13.3	40.2
Serine (or cysteine) proteinase inhibitor, clade H (heat shock protein 47), member 1	NM 004353	1.13	1.02	6.99	13.5	21.3
DnaJ (Hsp40) homolog, subfamily B, member 1	BG537255	1.09	2.35	9.83	11.4	14.2
Protein kinase H11	AF133207	−1.01	1.43	3.45	12.9	12.1
Heat shock 27-kDa protein 1	NM 001540	1	−1.07	3.72	5.76	9.32
Heat shock 105 kDa	NM 006644	1.06	1.67	4.99	5.61	8.12
Heat shock protein (hsp110 family)	NM 014278	−1.36	1	2.29	3.92	7.68
DnaJ (Hsp40) homolog, subfamily B, member 6	AF080569	−1.29	1.01	2.32	5.99	6.73
DnaJ (Hsp40) homolog, subfamily B, member 4	BG252490	−1.01	1.08	2.75	2.88	4.4
Metabolism						
Spermidine/spermine N1-acetyltransferase	NM 002970	1.13	1.1	3.7	10.4	8.25
Uridine phosphorylase	NM 003364	1.13	1.04	1.95	4.65	6.29
Carnitine palmitoyltransferase I	BF001714	1.07	−1.13	1.14	2.88	5.79
NADP-dependent malic enzyme, malate oxidoreductase	AL049699	−1.4	1.41	4.81	5.33	4.94
Carbonic anhydrase II	M36532	−1.15	1.19	1.74	4.87	4.75
6-Phosphofructo-2-kinase/fructose-2,6-biphosphatase 3	NM 004566	−1.04	1.21	1.28	5.76	4.45
Malic enzyme 1, NADP(+)-dependent, cytosolic	NM 002395	−1.23	1.25	4.33	5.62	4.28
Biliverdin reductase B (flavin reductase (NADPH))	NM 000713	−1.01	1.53	5.82	5.6	4.2
Cytochrome *c* oxidase assembly protein COX15	BC002382	1.91	1.58	1.29	4.92	3.95
Heme oxygenase (decycling) 1	NM 002133	−1.17	1.26	2.53	3.99	3.83

TABLE 2 (*continued*). Transcriptional Profiles of Bortezomib-Treated WERI-Rb1 Cells by Oligonucleotide Microarray Analysis

Gene Name	Accession No.	2 h	4 h	8 h	16 h	24 h
Glutathione peroxidase 3 (plasma)	NM 002084	1.02	1.69	3.7	2.82	3.37
Cystathionase (cystathionine gamma-lyase)	NM 001902	1.02	1.88	6.29	3.63	3.05
Galactosidase, alpha	NM 000169	1.19	1.4	2.67	3.32	3.04
Asparagine synthetase	NM 001673	1.11	1.56	4.8	2.63	−1.22
ATP synthase, H+ transporting, mitochondrial F0 complex, subunit c (subunit 9), isoform 1	AL080089	1.05	−1.3	−3.37	−6.19	−4.88
Metastasis						
Glycoprotein (transmembrane) nmb	NM 002510	−1.16	−1.03	−1.03	7.78	11.6
Putative transmembrane protein	NM 012342	−1.13	−1.04	1.73	8.69	7.78
Neuronal function						
Synaptosomal-associated protein, 23 kDa	BC003686	−1.04	−1.13	2.32	5.07	10.2
Purkinje cell protein 4	NM 006198	1.04	−1.33	1.67	4.22	5.82
Activity-regulated cytoskeleton-associated protein	AF193421	−1.03	1.04	−1.22	6.46	5.37
Arylalkylamine N-acetyltransferase	NM 001088	1.05	−1.33	−3.85	−7.76	−6.58
Protein synthesis and folding						
Mitochondrial ribosomal protein L18	NM 014161	−1.09	−1.01	2.54	4.67	6.46
Eukaryotic translation initiation factor 2-alpha kinase 3	NM 004836	1.06	−1.21	3.58	3.94	3.88
Peptidylprolyl isomerase D (cyclophilin D)	NM 005038	1.03	1.27	2.16	2.21	2.49
Cysteinyl-tRNA synthetase	NM 001751	1.02	1.29	2.49	2.4	1.27
Signaling						
Ras-related associated with diabetes	NM 004165	1.05	−1.15	2.82	27.4	24.1
Diphtheria toxin receptor (heparin-binding epidermal growth factor-like growth factor)	NM 001945	1.07	1.06	1.76	13.9	15.3
Adrenomedullin	NM 001124	1.14	1.25	2.06	19.2	14.3
Phosphoprotein regulated by mitogenic pathways	NM 025195	1.08	−1.14	1.86	11.4	8.48
Neuropeptide Y receptor Y1	NM 000909	−1.01	−1.24	1.68	5.06	7.41
Serum/glucocorticoid regulated kinase	NM 005627	−1.04	−1.33	1.43	8.09	7.23
Serum-inducible kinase	NM 006622	−1.15	−1.2	2.16	8.44	6.92
Dual-specificity phosphatase 6	BC003143	−1.13	−1.09	3.41	8.13	6.51
Dual-specificity phosphatase 4	NM 001394	−1.13	1.15	1.65	6.33	6.44
Dual-specificity phosphatase 1	NM 004417	1.16	1.51	3.65	8.66	6.12
Ras-induced senescence 1	BF062629	−1.06	−1.07	1.31	4.78	5.85
Vascular endothelial growth factor	AF022375	1.2	2.08	4.81	8.25	5.67
CD14 antigen	NM 000591	1.02	1.16	1.53	7.56	5.65
Interleukin 15	NM 000585	−1.18	−1.07	2.63	4.89	5.6
Phospholipase A2, group IVC (cytosolic, calcium-independent)	AF065214	−1.04	−1.02	1.18	5.63	5.59
Ephrin-B2	BF001670	1.04	−1.12	1.35	5.75	5.56
Dual-specificity phosphatase 8	NM 004420	1.08	1.05	3.69	11.3	5.42
CXCR4	AJ224869	1.06	−1.11	1.91	6.39	5.22
Stanniocalcin 2	AI435828	1.01	2.47	11.6	6.44	4.92
Ephrin-A1	NM 004428	1.12	1.18	1.06	7.53	4.73
EphA4	NM 004438	1.08	−1.26	1.44	3.82	4.47
Brain-derived neurotrophic factor	NM 001709	1.24	1.16	1.63	3.59	4.47
Calmodulin 1 (phosphorylase kinase, delta)	M27319	1.06	−1.08	1.38	3.32	4.41
Dual-specificity phosphatase 2	NM 004418	1.14	1.41	2.05	10.9	3.88
Tumor necrosis factor (ligand) superfamily, member 9	NM 003811	1.44	3.3	3.25	4.89	3.86
GAP-associated tyrosine phosphoprotein p62 (Sam68)	AW592227	1.12	1.18	1.75	4.73	3.82
Insulin receptor substrate 2	BF700086	1.21	1.18	2	4.72	3.65
PI-3 kinase-related kinase SMG-1	BG256504	1.02	1.17	1.53	2.34	2.93
Phosphoprotein C8FW	NM 021158	1.33	2.35	8.71	8.38	2.89
Dual-specificity phosphatase 5	U16996	−1	1.03	1.23	4.34	2.64
Mitogen-activated protein kinase kinase 3	NM 002756	1.04	1.21	1.13	3.03	2.18
GABA(A) receptors associated protein-like 3	AF180519	1.22	1.92	3.26	3.03	2.05
Tumor necrosis factor receptor superfamily, member 1A	NM 001065	1.06	1.62	2.04	2.01	1.53
PDZ-binding kinase; T-cell originated protein kinase	NM 018492	−1.03	−1.2	−2.1	−4.52	−4.6
Pleckstrin homology-like domain, family A, member 1 (TDAG51)	AA576961	−1.16	−1.08	−2.75	−5.64	−4.81
Guanine nucleotide binding protein (G protein), beta polypeptide 3	NM 002075	1.04	−1.1	−2.8	−8.57	−11.6
RAB26, member RAS oncogene family	NM 014353	1.21	−1.39	−5.87	−16.7	−17.3
Stress response						
Bcl-2-associated athanogene 3	NM 004281	−1.24	1.64	7.57	17.8	27.7
Growth arrest and DNA-damage-inducible, beta	NM 015675	−1.06	1.03	2.54	28.2	18.1
Protein phosphatase 1, regulatory (inhibitor) subunit 15A (*GADD34*)	U83981	1.13	1.79	2.03	7.66	7.79
Growth arrest and DNA damage inducible, gamma	NM 006705	1.34	1.4	1.23	2.61	2.84
Growth arrest and DNA damage inducible, alpha	NM 001924	1.02	1.43	1.77	3.09	2.35
HIF-1-responsive *RTP801*	NM 019058	1.5	5.24	5.13	3.21	1.91
Homocysteine-inducible, endoplasmic reticulum stress-inducible, ubiquitin-like domain member 1	AF217990	1.2	1.81	2.65	2.74	1.71
Transcription factors						
Inhibitor of DNA binding 2, dominant negative helix-loop-helix protein	NM 002166	−1.01	−1.2	1.54	12.3	17.9

TABLE 2 (*continued*). Transcriptional Profiles of Bortezomib-Treated WERI-Rb1 Cells by Oligonucleotide Microarray Analysis

Gene Name	Accession No.	2 h	4 h	8 h	16 h	24 h
c-fos	BC004490	−1	1.1	2.57	16.6	10.7
Endothelial PAS domain protein 1 (HIF-2a)	AF052094	−1.06	1.14	1.47	9.53	9.99
Kruppel-like factor 5 (intestinal)	AF132818	−1.13	−1.24	1.86	7.39	8.56
POU domain, class 3, transcription factor 1	NM 002699	1.04	−1.15	1.26	6.99	7.81
MafB	NM 005461	1.06	−1.03	1.05	9.35	7.45
Activating transcription factor 3	NM 001674	1.22	2.2	11.6	14.7	7.35
Zinc finger protein 277	AK027128	1.14	1.13	4.12	9.52	6.65
c-fosB	NM 006732	1.07	1.1	1.49	11.5	6.45
CCAAT/enhancer binding protein (C/EBP), delta	NM 005195	−1.02	−1.24	1.35	4.67	6.35
Distal-less homeobox 2	NM 004405	1.08	−1.09	1.23	6.51	5.8
Regulator of G-protein signaling 2 (RGS2)	NM 002923	1.06	1.23	1.57	4.14	5.52
Transcription factor 8	NM 030751	−1.1	−1.02	1.28	6.08	5.42
Early growth response 4	NM 001965	1.06	1.14	1.14	11.6	5.38
MafG	NM 002359	1.57	2.73	4.81	6.54	5.29
Kruppel-like factor 4 (gut)	NM 004235	−1.09	−1.07	1.39	5.9	5.19
Nuclear receptor subfamily 4, group A, member 2	AI935096	−1.09	−1.01	1.55	5.2	5.05
CCAAT/enhancer binding protein (C/EBP), beta	AL564683	1.41	2.95	6.96	8.3	4.91
cAMP-responsive element modulator	NM 001881	−1.06	1.27	2.54	4.8	4.15
Achaete-scute complex-like 1 (*Drosophila*)	BC002341	1.39	1.22	1.6	4.17	3.22
ets variant gene 5 (ets-related molecule)	BF060791	1.01	1.02	1.9	3.68	3.12
c-jun	BG491844	1.1	1.46	3.59	3.8	2.93
HIF1-beta	AF001307	1.66	1.42	1.45	3.3	2.49
Early growth response 1	NM 001964	1.03	1.02	1.51	4.26	2.23
DNA-damage-inducible transcript 3 (*GADD153*)	BC003637	1.36	2.31	3.71	3.59	2.21
X-box binding protein 1 (*XBP-1*)	NM 005080	1.16	2.09	3.15	1.44	1.65
Transporters						
Solute carrier family 7, (cationic amino acid transporter, y+ system) member 11	AB040875	1.08	3.91	32.4	21.4	9
Solute carrier family 5 (inositol transporters), member 3	AI867198	1.33	1.27	3.86	5.64	5.63
Solute carrier family 7 (cationic amino acid transporter, y+ system), member 5	AB018009	1	1.78	5.73	4.65	3.7
Chloride intracellular channel 1	AF034607	1.37	1.61	2.26	3.94	3.6
Solute carrier family 1 (glial high-affinity glutamate transporter), member 3	NM 004172	1.02	−1.01	1.75	3.25	3.24
Nuclear RNA export factor 1	BC004904	1.13	1.06	1.39	2.64	3.14
Solute carrier family 3 (activators of dibasic and neutral amino acid transport), member 2	NM 002394	1.09	1.77	2.61	2.87	2.89
Solute carrier family 1 (neutral amino acid transporter), member 5	AF105230	1.05	1.33	2.95	2.08	1.17
Solute carrier family 25 (mitochondrial carrier; dicarboxylate transporter), member 10	NM 012140	−1.03	−1.19	−1.73	−5.06	−4.89
Retinol binding protein 3, interstitial	J03912	−1.07	−1.22	−3.08	−5.92	−5.82
Cholinergic receptor, nicotinic, alpha polypeptide 1 (muscle)	NM 000079	−1.03	−1.18	−1.86	−5.69	−7.83
Ubiquitin/proteasome pathway						
Sequestosome 1	NM 003900	1.27	2.83	4.81	4.65	4.67
Similar to ubiquitin binding protein	NM 019116	−1.06	1.48	2.19	3.27	3.76
Proteasome (prosome, macropain) 26S subunit, non-ATPase, 12	AI446530	1.03	1.5	2.59	3.04	2.73
26S proteasome-associated pad1 homolog	NM 005805	1.06	1.7	2.53	2.81	2.49
Proteasome (prosome, macropain) 26S subunit, non-ATPase, 13	NM 002817	1.13	1.45	2.38	2.53	2.23
Proteasome (prosome, macropain) 26S subunit, non-ATPase, 11	BF432873	1.08	1.8	1.97	2.57	2.04
Proteasome (prosome, macropain) 26S subunit, ATPase, 1	NM 002802	1.14	1.45	2	2.1	1.98
Proteasome (prosome, macropain) 26S subunit, ATPase, 6	NM 002806	1.2	1.56	2.26	2.15	1.95
Proteasome (prosome, macropain) subunit, alpha type, 5	NM 002790	1.1	1.61	2.2	1.73	1.93
Proteasome (prosome, macropain) 26S subunit, non-ATPase, 7	NM 002811	1.22	1.61	2.02	1.96	1.89

Shows selected known genes whose transcripts demonstrated the most prominent change on treatment of WERI-Rb1 cells with bortezomib (25 nM for 2, 4, 8, 16, and 24 hours). Numbers represent fold change in expression compared with vehicle-treated controls harvested at the same time point.

cell lines and was similar to other types of malignancies, such as multiple myeloma, we have treated with bortezomib.[19]

More specifically, we found that bortezomib targets transcripts with prominent roles in cell growth and apoptosis signaling. Specifically, bortezomib upregulated the proapoptotic Bcl-2 family members *Noxa* (also known as PMA-induced protein 1 [*PMAIP1*] and implicated in mediating apoptosis induced by cellular stress, DNA damage, and p53 activation, resulting in the activation of caspase-9[28]), *PUMA*, and harakiri and serine/threonine protein kinase 17A (*STK17A*, also known as DAP kinase-related apoptosis-inducing protein kinase 1), which induces apoptosis.[29,30] Moreover, bortezomib suppressed the transcript for the inhibitor of apoptosis survivin. This transcriptional profile could contribute to the induction of apoptosis by bortezomib.

Furthermore, bortezomib potently triggered the transcription of genes related to ubiquitin-proteasome function (such as several proteasome subunits) and molecular chaperones of the HSP family (*HSP70, HSP27, HSP40, HSP47*). It is possible that these changes represent a stress response because bortezomib-treated tumor cells unsuccessfully attempt to compensate for the loss of proteasome activity by synthesizing new proteasomes (to restore proteasome activity) and new chaperones (to keep proteins in the correct conformation and lessen the need

TABLE 3. Transcriptional Profiles of Bortezomib-Treated Y79 Cells by Oligonucleotide Microarray Analysis

Gene Name	Accession No.	2 h	4 h	8 h	16 h	24 h
Adhesion						
Cell membrane glycoprotein (adhesion regulating molecule 1 [*ADRM1*])	NM 007002	1.19	1.33	2.07	2.29	2.71
Intercellular adhesion molecule 2	NM 000873	1.03	1	1.75	2.6	1.71
Neural cell adhesion molecule 1	AA126505	1.09	1.27	−1.46	−4.8	−2.14
Apoptosis						
TSSC3	AF001294	1.15	1.02	1.74	4.18	13.7
Clusterin	AI982754	1.2	−1.42	3.72	4.48	13.5
Serine/threonine kinase 17a	AW194730	1.17	1.11	2.75	1.93	3.99
Harakiri, Bcl-2 interacting protein	NM 003806	1.17	1.09	1.8	2.2	3.16
Bcl-2 binding component 3 (*PUMA*)	AF332558	−1.12	1.17	1.88	1.95	2.92
Phosphatidylserine receptor	AA351360	1.05	1.1	1.54	1.57	2.69
Phorbol-12-myristate-13-acetate-induced protein 1 (*NOXA*)	NM 021127	1.16	1.2	2.99	3.01	2.46
Tumor necrosis factor receptor superfamily, member 10b (*TRAIL-R2*)	AF016266	−1.07	−1.1	1.29	1.93	2.12
Caspase 3, apoptosis-related cysteine protease	NM 004346	−1.01	−1.12	1.09	1.63	2.11
BH3 interacting domain death agonist (*Bid*)	NM 001196	1	−1.18	−1	4.03	1.16
Baculoviral IAP repeat-containing 5 (survivin)	AB028869	−1.15	−1.24	−1.65	−2.39	−3.11
Cell cycle						
Pregnancy-induced growth inhibitor	NM 013370	−1.02	1.28	2.73	2.78	5.61
Pelota homolog	NM 015946	1.23	1.97	2.65	2.59	3.89
Retinoblastoma binding protein 2	NM 005056	1.01	−1.68	2.02	1.35	2.86
Cyclin-dependent kinase inhibitor IC (p57, Kip2)	R78668	1.03	−1.06	−1.42	−1.03	2.29
Cyclin G2	L49506	−1.04	−2.03	−1.7	−2.58	−2
Cyclin-dependent kinase inhibitor 3 (CDK2-associated dual-specificity phosphatase)	AF213033	−1.05	−1.32	−1.48	−3.09	−2.02
Cyclin B2	NM 004701	−1.1	−1.2	−1.67	−1.35	−2.46
Putative c-Myc-responsive	AF040105	−1.05	−1.01	−1.63	−1.26	−2.64
Cyclin A2	NM 001237	−1.28	−1.11	−1.61	−1.32	−2.79
Serine/threonine kinase 12 (Aurora kinase B)	AB011446	1.07	−1.06	−1.76	−2.66	−3.93
Cytoskeleton						
Stathmin-like 4	NM 030795	1.08	1.07	1.27	1.07	4.5
Syndecan binding protein (syntenin)	NM 005625	−1.02	1.03	1.91	−1.18	3.5
Microtubule-associated protein 1A	AW296788	1.17	3.18	3.34	2.25	3.3
Neurofilament 3 (150-kDa medium)	NM 005382	1.09	1.42	1.8	1.17	3.11
Differentiation						
msh homeobox homolog 1	NM 002448	1.14	−1.33	1.68	1.72	4.14
Cellular retinoic acid binding protein 1	NM 004378	1.24	−1.05	−1.53	−4.09	−2.68
Doublecortex; lissencephaly, X-linked (doublecortin)	NM 000555	1.05	−1.17	−1.96	−2.15	−5.98
DNA/RNA metabolism and function						
BRF2, subunit of RNA polymerase III transcription initiation factor, BRF1-like	NM 018310	1.4	2.49	2.71	3.37	3.61
Eukaryotic translation initiation factor 2-alpha kinase 3	NM 004836	1.05	−1.15	1.61	1.42	2.67
Transcription termination factor, RNA polymerase 1	AI632304	−1.02	−1.18	1.42	2.12	2.28
Eukaryotic translation initiation factor 5	NM 001969	−1.01	−1.31	2.24	2.65	2.22
Splicing factor, arginine/serine-rich 10 (transformer 2 homolog, *Drosophila*)	U87836	1	−1.34	2.38	2.89	2.08
Eukaryotic translation initiation factor 3, subunit 1 (alpha, 35 kDa)	AL031313	1.15	−1.27	2.43	2.43	1.74
H1 histone family, member 2	BC002649	1.14	−1.02	−1.65	−4.45	−1.84
Polymerase (RNA) II (DNA directed) polypeptide L (7.6 kDa)	BC005903	1.13	−1.11	−1.81	−4.76	−2.36
Topoisomerase (DNA) II alpha (170 kDa)	AL561834	1.09	−1.23	−1.36	−2.52	−3.42
Endonuclease G	NM 004435	1.02	−1.26	−2.1	−1.81	−3.84
X-ray repair complementing defective repair in Chinese hamster cells 4	BC005259	−1.05	−1.11	−2.31	−1.22	−4.02
Extracellular matrix						
Tuftelin 1	NM 020127	1.07	1.01	1.35	1.02	4.1
Collagen, type 1, alpha 1	K01228	1.01	1.13	−1.18	−3.83	3.33
Procollagen-proline, 2-oxoglutarate 4-dioxygenase (proline 4-hydroxylase), alpha polypeptide II	NM 004199	1.05	−1.09	1.66	1.82	3.19
Heat shock proteins						
Heat shock 70-kDa protein 1A	NM 005345	−1	1.15	12	12.2	40.4
Heat shock 70-kDa protein 6 (*HSP70B′*)	NM 002155	1.02	1.18	6.37	23.9	28.6
Heat shock 70-kDa protein 1B	NM 005346	−1.05	1.43	7.98	9.87	19.6
Protein kinase HI 1 (heat shock 27-kDa protein 8)	AF133207	1.03	1.03	3.62	4.18	9.52
Crystallin, alpha B	AF007162	−1.03	−1.08	1.17	2.91	9.45
Serine (or cysteine) proteinase inhibitor, clade H (heat shock protein 47), member 1	NM 004353	−1.04	1.08	3.44	7.28	8.98
Heat shock 27-kDa protein 1	NM 001540	1.09	−1.01	3.2	6.07	7.83
DnaJ (*Hsp40*) homolog, subfamily B, member 1	BG537255	1.14	1.17	5.63	5.52	7.67
Heat shock 105 kDa	BG403660	1.01	1.11	4.23	6.93	5.65
Heat shock protein (hsp110 family)	NM 014278	1.1	−1.21	2.02	1.93	2.77
DnaJ (*Hsp40*) homolog, subfamily B, member 6	AF080569	−1.13	−1.17	1.96	1.98	2.59
DnaJ (*Hsp40*) homolog, subfamily B, member 2	NM 006736	1.3	1.19	1.37	1.31	2.2

TABLE 3 (*continued*). Transcriptional Profiles of Bortezomib-Treated Y79 Cells by Oligonucleotide Microarray Analysis

Gene Name	Accession No.	2 h	4 h	8 h	16 h	24 h
Metabolism						
Heme oxygenase (decycling) I	NM 002133	−1.15	1.4	2.27	1.57	4.44
Spermidine/spermine N1-acetyltransferase	BE971383	1.19	−1.22	1.49	1.75	4.43
NAD(P)H dehydrogenase, quinone 2	NM 000904	1.18	1.03	3.17	1.19	4.41
Uridine phosphorylase	NM 003364	1.31	−1.03	2.53	6.31	4.3
Galactosidase, alpha	NM 000169	1.12	1.22	2.85	1.75	4.17
Cytochrome *c* oxidase assembly protein COX15	BC002382	−1.19	1.98	−1.68	2.21	3.86
Biliverdin reductase B (flavin reductase [NADPH])	NM 000713	1.19	1.01	3.16	−2.29	3.66
ATPase, class I, type 8B, member 1	BG252666	−1.18	1.33	1.46	1.91	3.6
Carbonyl reductase 3	NM 001236	−1.01	−1.19	1.38	2.63	3.56
Glutamate-cysteine ligase, modifier subunit	NM 002061	−1.26	1.85	1.97	2.32	3.36
Glutathione peroxidase 3 (plasma)	AW149846	−1	1.26	2.14	1.28	3.17
NAD(P)H dehydrogenase, quinone 1	BC000906	1.02	1.06	1.8	5.85	2.71
Cystathionase (cystathionine gamma-lyase)	NM 001902	1.06	1.18	5	2.11	2.06
Asparagine synthetase	NM 001673	1.04	1.07	2.21	2.53	1.84
ATP synthase, H+ transporting, mitochondrial F0 complex, subunit c (subunit 9) isoform 3	NM 001689	−1.07	−1.11	−1.51	−2.39	−1.48
Amylo-1,6-glucosidase, 4-alpha-glucanotransferase	NM 000645	1.05	−1.31	−1.24	−2.73	−3.71
Retinol binding protein 3, interstitial	J03912	1.21	−1.21	−2.42	−1.35	−5.64
Signaling						
Dual-specificity phosphatase 4	BC002671	1.17	−1.32	1.31	5.82	7.85
Ras-related associated with diabetes	NM 004165	1.53	−1.33	2.6	7.68	7.81
Adrenomedullin	NM 001124	1.12	1.09	1.39	2.36	6.15
Ephrin-B2	U16797	1.38	−1.35	1.25	−1.46	4.27
Tumor necrosis factor (ligand) superfamily, member 9	NM 003811	1.38	2.33	2.6	1.91	4.21
Dual-specificity phosphatase 1	NM 004417	1.29	1.2	1.71	3.05	3.98
GABA(A) receptor-associated protein-like 3	AF180519	−1.19	1.57	2.13	2.5	3.9
CXCR4	AJ224869	1.29	−1.1	1.6	−1.05	3.56
Lymphoid blast crisis oncogene	NM 006738	−1.33	1.79	−1.71	2.11	3.53
GTP binding protein overexpressed in skeletal muscle	NM 005261	1.4	−1.16	1.01	−1.2	3.5
Dual-specificity phosphatase 8	NM 004420	1.23	−1.12	1.69	2.14	3.37
Serum-inducible kinase	NM 006622	1.11	−1.32	1.53	2.08	3.23
Stanniocalcin 2	AI435828	1.14	1.71	3.98	3.15	3.2
GABA(A) receptor-associated protein-like 1	AF087847	−1.52	1.49	2.62	3.01	3.17
Serum/glucocorticoid-regulated kinase	NM 005627	1.04	−1.41	−1.1	−1.64	3
PI-3 kinase-related kinase SMG-1	BG256504	1.07	1.33	1.37	2.33	2.94
Insulin receptor substrate 2	BF700086	1	1.29	1.46	2.33	2.7
Mitogen-activated protein kinase kinase 3	AA780381	1.18	1.09	1.1	1.09	2.58
EphA2	NM 004431	1.02	−1.04	1.17	2.04	2.49
Transducer of ERBB2, 2	D64109	1.24	−1.91	1.3	1.29	2.49
Vascular endothelial growth factor	H95344	1.14	1.28	2.21	2.36	2.33
Ras-induced senescence 1	BF062629	−1.02	1.06	−1.29	1.13	2.33
Ras association (RalGDS/AF-6) domain family 2	NM 014737	−1.2	1.17	−1.66	−1.1	2.26
TDAG51/IPL homolog 1 (TIH1)	NM 012396	1.16	1.01	1.23	3.8	2.14
Inhibin, beta E	BC005161	1.19	1.44	3.82	6.85	1.83
Phospholipase A2-activating protein	AF145020	1.02	1.44	2.29	2.85	1.81
Neurturin	AL161995	1.09	−1.4	−1.34	−3.42	−1.77
Mitogen-activated protein kinase kinase 6	NM 002758	1.15	−1.07	−1.86	−4.22	−1.89
Stromal cell derived factor receptor 1	NM 017455	−1.1	−1.06	−1.2	−2.84	−1.94
Serine/threonine kinase 15	NM 003600	−1.24	−1.26	−1.52	−1.12	−2.45
Serine/threonine kinase 6	NM 003158	−1.3	−1.21	−1.4	−1.03	−2.55
Downregulated in ovarian cancer 1	NM 014890	−1.13	−1.5	−1.84	−2.73	−2.86
PDZ-binding kinase; T-cell originated protein kinase	NM 018492	1.04	−1.37	−1.42	−2.14	−2.87
Ca2+-promoted Ras inactivator	AB011110	−1.03	1.15	−1.87	−2.24	−3.31
Phosphatidylinositol glycan, class F	NM 002643	1.03	−1.18	−1.16	−3.7	−3.31
S-phase kinase-associated protein 2 (p45)	BC001441	1.02	−1.22	−1.14	1.01	−3.63
Somatostatin receptor 2	AF184174	1.02	−1.26	−2.28	−2.32	−3.89
Neurotrophic tyrosine kinase, receptor, type 1	NM 002529	1.18	−1.07	−1.46	−3.19	−4.41
RAB26, member RAS oncogene family	AI690165	1.17	−1.13	−2.85	−3.76	−4.73
Guanine nucleotide binding protein (G protein), beta polypeptide 3	NM 002075	−1.04	−1.02	−2.14	−1.36	−4.83
Cdc42 guanine exchange factor (GEF) 9	NM 015185	−1.08	−1.04	−1.76	−2.88	−6.32
Guanine nucleotide binding protein (G protein), gamma transducing activity polypeptide 1	NM 021955	1.05	−1.59	−2.01	−1.04	−10.7
Stress response						
Bcl-2-associated athanogene 3 (*BAG3*)	NM 004281	1.18	1.14	5.37	2.67	11.5
Growth arrest and DNA damage inducible, beta	AF078077	1.07	−1.18	1.24	2.85	5.69
Protein phosphatase 1, regulatory (inhibitor) subunit 15A (*GADD34*)	U83981	1.45	1.63	2.16	4.11	5.34
Growth arrest and DNA damage inducible, alpha (*GADD45A*)	NM 001924	1.17	1.4	1.76	2.56	3.45
Homocysteine-inducible, endoplasmic reticulum stress-inducible, ubiquitin-like domain member 1	AF217990	1.15	1.26	2.34	2.45	2.32

TABLE 3 (*continued*). Transcriptional Profiles of Bortezomib-Treated Y79 Cells by Oligonucleotide Microarray Analysis

Gene Name	Accession No.	2 h	4 h	8 h	16 h	24 h
HIF-1 responsive *RTP801*	NM 019058	1.27	2.11	3.69	3.59	2.19
Growth arrest and DNA damage inducible, gamma (*GADD45G*)	NM 006705	1.23	1.18	1.75	2.78	1.88
Transcription factors						
Zinc finger protein 277	AK027128	1.05	−1.32	2.84	4.89	16.2
Activating transcription factor 3	NM 001674	1.5	1.4	6	6.06	10.3
MafF	AL021977	1.56	1.78	4.17	9.41	8.19
Inhibitor of DNA-binding 2, dominant-negative helix-loop-helix protein	AI819238	1.5	−1.01	1.08	3.63	8.05
Kruppel-like factor 5 (intestinal)	AF132818	1.05	1.01	1.39	2.9	6.69
c-jun	NM 002228	1.78	−1.22	4.89	4.39	6.37
Kruppel-like factor 4 (gut)	BF514079	1.3	−1.05	1.44	4.24	6.32
c-fos	BC004490	1.64	1.23	1.88	2.89	5.8
Regulator of G-protein signaling 2, 24 kDa	NM 002923	1.23	1.14	1.8	2.25	4.79
DNA damage inducible transcript 3 (*GADD153*)	BC003637	1.16	1.77	2.96	3.91	4.08
Activating transcription factor 5	BC005174	1.26	1.08	1.91	6.34	3.97
Kruppel-like factor 2 (lung)	NM 016270	1.24	−1.05	−1.1	2.43	3.97
CCAAT/enhancer binding protein (C/EBP), beta	AL564683	1.11	1.54	3.31	2.45	3.75
ets variant gene 5 (ets-related molecule)	NM 004454	−1.01	1.23	1.97	2.4	3.68
POU domain, class 3, transcription factor 1	NM 002699	1.19	−1.33	1.02	1.11	3.56
Endothelial PAS domain protein 1 (HIF-2a)	AF052094	1.06	−1.02	1.1	−2.99	3.55
MafG	NM 002359	1.05	2.84	2.08	4.56	3.4
c-fosB	NM 006732	1.27	1.14	1.03	1.94	2.54
X-box binding protein 1 (*XBP-1*)	NM 005080	1.1	1.35	2.63	2.39	1.69
CCAAT/enhancer binding protein (C/EBP), gamma	NM 001806	1.09	−1.09	2.32	2.8	1.21
c-*myc* binding protein	D50692	−1.05	−1.24	−1.44	−2.6	−1.79
Thyroid hormone receptor interactor 7	AF274949	−1.03	−1.08	−1.73	−2.53	−1.98
POU domain, class 4, transcription factor 2	NM 004575	−1.04	−1.51	−1.66	−2.19	−3.05
Retinoid X receptor, gamma	NM 006917	1.04	−1.03	−2.08	−1.48	−3.63
Transporters						
Solute carrier family 7, (cationic amino acid transporter, y+ system) member 11	AB040875	−1.23	1.73	9.06	11.2	7.39
Chloride intracellular channel 1	AF034607	1.05	1.28	2.31	2.25	5.35
Solute carrier family 5 (inositol transporters), member 3	AI867198	1.07	1.1	1.61	1.89	3.29
Solute carrier family 3 (activators of dibasic and neutral amino acid transport), member 2	NM 002394	1.1	1.15	2.32	3.09	3.21
Solute carrier family 1 (glial high affinity glutamate transporter), member 3	NM 004172	1.12	1.01	1.44	2.12	3.15
Multidrug resistance-associated protein 5	AF146074	−1.1	1.1	1.49	2.05	2.87
Solute carrier family 4, sodium bicarbonate cotransporter, member 7	NM 003615	−1.23	−1.5	1.69	1.77	2.47
Solute carrier family 7 (cationic amino acid transporter, y+ system), member 5	AB018009	1.05	1.24	2.32	1.9	1.8
Lectin, mannose-binding, 1	NM 005570	−1.14	−1.38	−1.09	−1.93	−2.13
Neuronal pentraxin I	NM 002522	−1	−1.06	−2.21	−1.02	−2.78
Ubiquitin/proteasome pathway						
Sequestosome 1	NM 003900	1.02	1.23	2.05	3.17	3.34
26S proteasome-associated padI homolog	NM 005805	1.02	1.12	1.82	2.12	2.12
Proteasome (prosome, macropain) 26S subunit, ATPase, 4	NM 006503	1.12	1.21	1.79	1.96	2.09
Proteasome (prosome, macropain) 26S subunit, non-ATPase, 13	NM 002817	1.49	−1.04	2.02	1.28	2.03
Proteasome (prosome, macropain) 26S subunit, non-ATPase, 11	AF001212	−1.02	1.26	1.83	2.36	1.98
Ubiquitin carrier protein	NM 014501	−1.02	−1.17	−1.45	−2.17	−1.6
Ubiquitin-conjugating enzyme E2C	NM 007019	−1.06	−1.03	−1.55	−1.69	−2.3

Shows selected known genes whose transcripts demonstrated the most prominent change on treatment of Y79 cells with bortezomib (25 nM for 2, 4, 8, 16, and 24 hours). Numbers represent fold change in expression compared with vehicle-treated controls harvested at the same time point.

for proteasomal degradation). HSPs are induced in response to various stress stimuli, such as heat shock, oxidative free radicals, metal ions, and toxins. The human *HSP70* or *HSPA* multigene family comprises several highly conserved 70-kDa proteins required for cancer cell growth and survival.[31] The HSP70–1 (*HSPA1A*) and HSP70–2 (*HSPA1B*) coding sequences differ by 8 bp that do not alter the derived amino acid sequence and are not interrupted by introns.[32] HSP70 binds to the 3-prime untranslated region of mRNAs for cytokines and protooncogenes and protects them from degradation, thus exerting an antiapoptotic function.[33] Another transcript upregulated by bortezomib was the transcript for Bcl-2–associated athanogene (*BAG*)-3, a stress-inducible protein that interacts with the heat shock proteins 70, regulates chaperone protein activities, and promotes cell survival by enhancing the antiapoptotic effect of Bcl-2.[34]

We detected increased *Jun* and Fos mRNA and increased total and phospho-Jun protein levels in bortezomib-treated retinoblastoma cells, suggesting an involvement of the JNK (stress-activated protein kinase [SAPK])/AP-1 pathway in the stress response to NF-κB inhibition. Also found to be induced by bortezomib in our study were other stress pathway mediators, such as growth arrest- and DNA damage-inducible gene alpha (*GADD45A*, a stress-induced nuclear protein involved in growth arrest and DNA repair[35]) and DNA damage-inducible transcript 3, also known as growth arrest- and DNA damage-

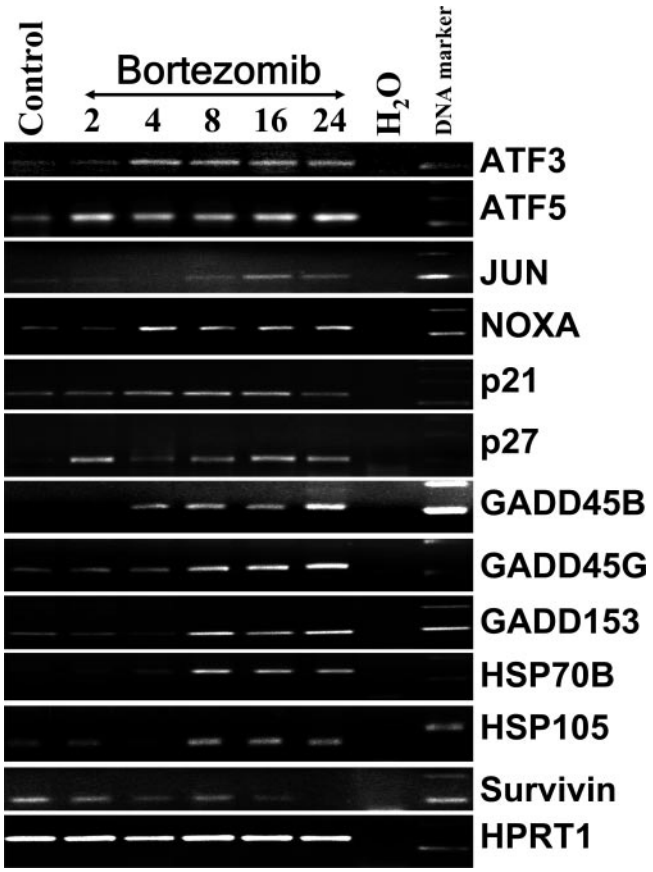

FIGURE 3. Changes in gene expression induced by bortezomib in retinoblastoma cells, as documented by RT-PCR and agarose gel electrophoresis. Modulation of expression of genes related to stress response, growth inhibition, and apoptosis induction in bortezomib-treated Y79 cells (25 nM for 2, 4, 8, 16, and 24 hours). Expression changes observed for these selected genes with RT-PCR were in agreement with the expression profiling results. The housekeeping gene was hypoxanthine guanine phosphoribosyltransferase 1 (*HPRT1*).

inducible gene (*GADD153*), a member of the CAAT/enhancer binding protein (C/EBP) family of transcription factors capable of triggering growth arrest and apoptosis.[36] The latter is known to be induced by AP-1,[37] hypoxia,[38] proteasome inhibition,[39] and endoplasmic reticulum (ER) stress.[40] Because ER is the site of synthesis and folding of secretory proteins, ER dysfunction affects protein folding, leading to high load of misshapen proteins that must be degraded through the ubiquitin–proteasome pathway. Conversely, the inhibition of proteasome activity results in ER stress. When ER function is severely impaired, *GADD153* plays a key role in triggering apoptosis,[40] together with the JNK/Jun pathway and caspase-12,[41] which were also found to be activated by bortezomib in our study. In addition, two other members of the C/EBP family, C/EBPβ and C/EBPγ, were induced by bortezomib in our study.

Another transcription factor modulated by bortezomib in our model was activating transcription factor 3 (ATF3), a member of the mammalian activation transcription factor/cAMP responsive element-binding (CREB) protein family of transcription factors and an immediate early response gene induced in cells exposed to a variety of stress stimuli, including ER stress[42] and proteasome inhibition.[39,43] ATF3 frequently functions as a complex with *GADD153*.[42] ATF3 plays a critical role in accelerating caspase activation and apoptosis in response to chemo-

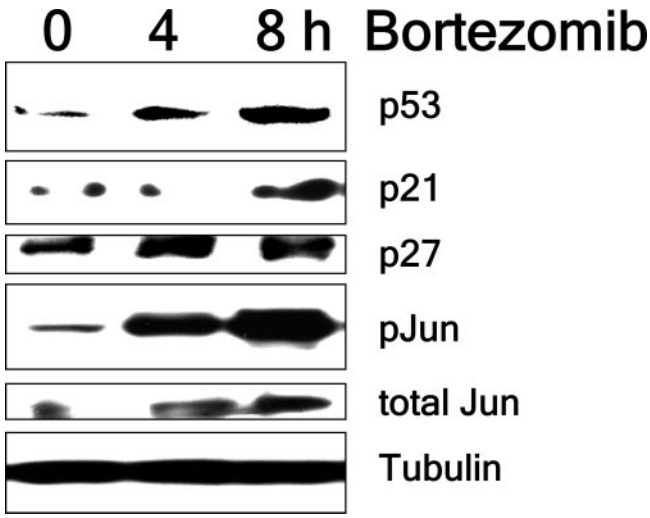

FIGURE 4. Bortezomib increases the levels of p53, p21, p27, and Jun proteins in retinoblastoma cells. WERI-Rb1 cells were treated with bortezomib (25 nM) for 0 to 16 hours. Total cell lysates were assayed by immunoblotting for the presence of p53 and p21. Bortezomib increased the expression of p53, p21, and p27 proteins and the presence of phosphorylated and total c-Jun. Tubulin is shown as a loading control.

therapeutic and noxious agents.[44–47] ATF3 induces another stress response gene, growth arrest and DNA damage inducible gene *GADD34* (also known as protein phosphatase 1 regulatory [inhibitor] subunit 15A (PPP1R15A)),[48] which was also upregulated by bortezomib in our study.

Finally, other prominent bortezomib-induced expression pattern changes involved extracellular matrix and adhesion

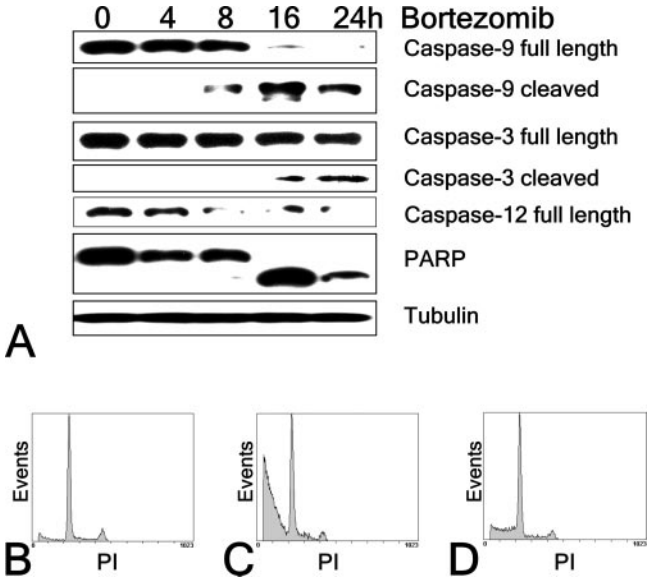

FIGURE 5. Functional involvement of caspases in apoptosis induced by proteasome inhibition. (**A**) WERI-Rb1 cells were treated with bortezomib (25 nM) for 0 to 16 hours. Total cell lysates were assayed by immunoblotting for caspase levels. Bortezomib (25 nM) induced the cleavage of caspase-9, caspase-3, and caspase-12. The caspase substrate PARP was also found to be cleaved. (**B–D**) The cell cycle profile of bortezomib-treated Y79 cells was evaluated by propidium iodide (PI) analysis and flow cytometry. The pan-caspase inhibitor ZVAD-FMK attenuated bortezomib-induced apoptosis in Y79 cells, as demonstrated by PI staining. (**B**) DMSO control. (**C**) Bortezomib (25 nM for 24 hours). (**D**) 25 nM for 24 hours + ZVAD-FMK (20 μM).

molecules, solute carriers, and transport proteins. Bortezomib increased p53, p21, and p27 protein levels in retinoblastoma cells. p53 is an additional proteasome substrate, and proteasome inhibition stabilizes p53 protein levels.[7,8] The *p21* gene is a transcriptional target of p53, and the p21 protein is also degraded by the proteasome,[49] thus suggesting two possible mechanisms for the upregulation of p21 protein levels (transcriptional and posttranslational). These findings may support a p53/p21-mediated signaling pathway for growth arrest and apoptosis induced by proteasome inhibitors.[7] It should be pointed out, however, that proteasome inhibitors are effective in inducing apoptosis even in tumor cells that lack functional p53.

Bortezomib induced caspase-dependent apoptosis in retinoblastoma cells. Cleavage of caspases-9, -3, and -12 was found (retinoblastoma cells do not express caspase-8 because of epigenetic gene silencing by overmethylation[50]), and caspase inhibition protected retinoblastoma cells from bortezomib-induced apoptosis, thus confirming the role of the caspase cascade in our model. Finally, bortezomib sensitized retinoblastoma cells to sublethal concentrations of conventional DNA-damaging chemotherapeutic agents, such as doxorubicin, in agreement with similar results in other malignancies.[20,21] A synergistic interaction has also been reported for the combination of the chemotherapeutic agent camptothecin with the proteasome inhibitor MG132 in Y79 cells.[51] These findings suggest that bortezomib may be incorporated in chemotherapy protocols and used as a chemosensitizer. This approach is under investigation in other malignancies, and a recent phase 1 trial of bortezomib combined with liposomal doxorubicin in patients with advanced hematologic malignancies showed that the combination was safely administered and had enhanced antitumor activity.[52]

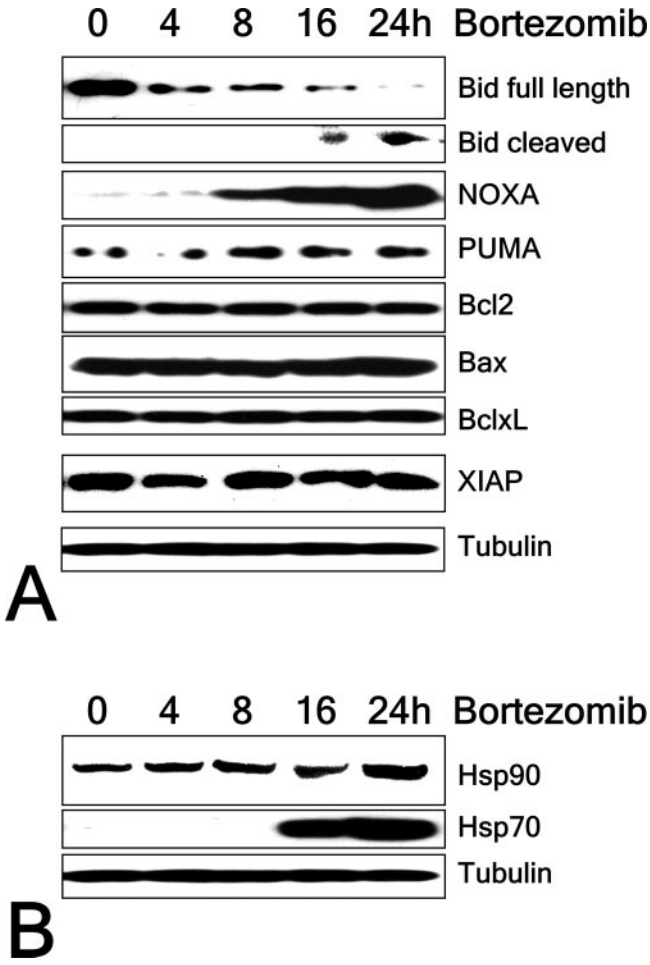

FIGURE 6. Involvement of Bcl-2 and HSP family members in bortezomib-induced cell death in retinoblastoma cells. (**A**) Bortezomib (25 nM) induced the cleavage of Bid in WERI-Rb1 cells, a member of the Bcl-2 family, which, on cleavage, translocated to the mitochondria to promote apoptosis. In addition, bortezomib upregulated the expression of the proapoptotic Bcl-2 family members Noxa and PUMA. Tubulin is shown as a loading control. (**B**) Bortezomib (25 nM) strongly upregulated HSP70 protein levels (very short film exposure shown) and induced a less pronounced increase in HSP90 levels. Tubulin is shown as a loading control.

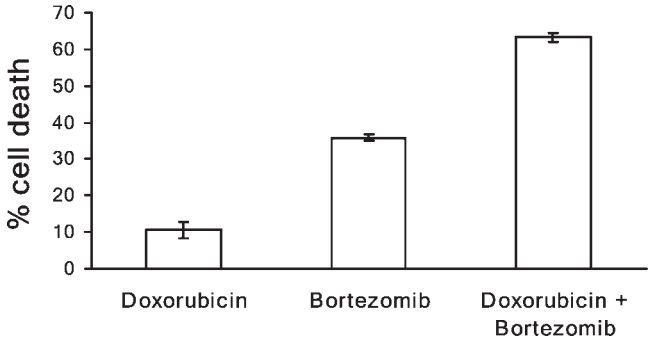

FIGURE 7. Sensitizing effect of bortezomib to conventional cytotoxic chemotherapy in retinoblastoma cells. WERI-Rb1 cells were treated with a low dose of doxorubicin (0.05 μg/mL) for 48 hours. During the last 24 hours of that treatment, the cells were also exposed to bortezomib (5 nM) or vehicle. At the end of the 48-hour incubation, the percentage of cell death (mean $\pm$ SD) was quantified by MTT. Cell death was 10.6% $\pm$ 2.2% in cells treated with doxorubicin alone, 35.8% $\pm$ 0.9% in cells treated with bortezomib alone, and 63.2% $\pm$ 1.3% in cells treated with the combination. Each experimental condition was repeated at least in triplicate wells. Data reported are mean $\pm$ SD of representative experiments. Combined treatment with bortezomib had a sensitizing effect on doxorubicin-induced cell death.

In summary, we have characterized the molecular signature of bortezomib treatment in two retinoblastoma cell lines and defined apoptotic pathways triggered by this novel anticancer agent. Our study shows that bortezomib suppresses proliferation and cell survival pathways, activates apoptotic and stress pathways, and stimulates transcription of components of the proteasome/ubiquitin and HSP pathways in retinoblastoma cell lines in vitro. Given that the two studied retinoblastoma cell lines have been grown for several years in tissue culture, it may be that they have accumulated additional genetic or epigenetic events and no longer fully recapitulate retinoblastoma pathophysiology. Therefore, additional work in animal models is necessary before clinical trials are initiated in pediatric patients with retinoblastoma.

References

1. Ciechanover A, Finley D, Varshavsky A. The ubiquitin-mediated proteolytic pathway and mechanisms of energy-dependent intracellular protein degradation. *J Cell Biochem*. 1984;24:27–53.
2. Ciechanover A, Finley D, Varshavsky A. Ubiquitin dependence of selective protein degradation demonstrated in the mammalian cell cycle mutant ts85. *Cell*. 1984;37:57–66.
3. Varshavsky A, Bachmair A, Finley D, Gonda DK, Wunning I. Targeting of proteins for degradation. *BioTechnology*. 1989;13:109–143.
4. Varshavsky A. The ubiquitin system. *Trends Biochem Sci*. 1997; 22:383–387.

5. Hideshima T, Richardson P, Chauhan D, et al. The proteasome inhibitor PS-341 inhibits growth, induces apoptosis, and overcomes drug resistance in human multiple myeloma cells. *Cancer Res*. 2001;61:3071–3076.
6. Kubbutat MH, Jones SN, Vousden KH. Regulation of p53 stability by Mdm2. *Nature*. 1997;387:299–303.
7. Lopes UG, Erhardt P, Yao R, Cooper GM. p53-dependent induction of apoptosis by proteasome inhibitors. *J Biol Chem*. 1997;272: 12893–12896.
8. Shinohara K, Tomioka M, Nakano H, Tone S, Ito H, Kawashima S. Apoptosis induction resulting from proteasome inhibition. *Biochem J*. 1996;317(pt 2):385–388.
9. Meriin AB, Gabai VL, Yaglom J, Shifrin VI, Sherman MY. Proteasome inhibitors activate stress kinases and induce HSP72: diverse effects on apoptosis. *J Biol Chem*. 1998;273:6373–6379.
10. Adams J. The development of proteasome inhibitors as anticancer drugs. *Cancer Cell*. 2004;5:417–421.
11. Adams J. The proteasome: a suitable antineoplastic target. *Nat Rev Cancer*. 2004;4:349–360.
12. Richardson PG, Barlogie B, Berenson J, et al. A phase 2 study of bortezomib in relapsed, refractory myeloma. *N Engl J Med*. 2003; 348:2609–2617.
13. Dou QP, Goldfarb RH. Bortezomib (Millennium Pharmaceuticals). *IDrugs*. 2002;5:828–834.
14. Davis NB, Taber DA, Ansari RH, et al. Phase II trial of PS-341 in patients with renal cell cancer: a University of Chicago phase II consortium study. *J Clin Oncol*. 2004;22:115–119.
15. Goy A, Younes A, McLaughlin P, et al. Phase II study of proteasome inhibitor bortezomib in relapsed or refractory B-cell non-Hodgkin's lymphoma. *J Clin Oncol*. 2005;23:667–675.
16. Kondagunta GV, Drucker B, Schwartz L, et al. Phase II trial of bortezomib for patients with advanced renal cell carcinoma. *J Clin Oncol*. 2004;22:3720–3725.
17. Shah MH, Young D, Kindler HL, et al. Phase II study of the proteasome inhibitor bortezomib (PS-341) in patients with metastatic neuroendocrine tumors. *Clin Cancer Res*. 2004;10:6111–6118.
18. Papandreou CN, Daliani DD, Nix D, et al. Phase I trial of the proteasome inhibitor bortezomib in patients with advanced solid tumors with observations in androgen-independent prostate cancer. *J Clin Oncol*. 2004;22:2108–2121.
19. Mitsiades N, Mitsiades CS, Poulaki V, et al. Molecular sequelae of proteasome inhibition in human multiple myeloma cells. *Proc Natl Acad Sci USA*. 2002;99:14374–14379.
20. Mitsiades CS, McMillin D, Kotoula V, et al. Antitumor effects of the proteasome inhibitor bortezomib in medullary and anaplastic thyroid carcinoma cells in vitro. *J Clin Endocrinol Metab*. 2006;91: 4013–4021.
21. Mitsiades N, Mitsiades CS, Richardson PG, et al. The proteasome inhibitor PS-341 potentiates sensitivity of multiple myeloma cells to conventional chemotherapeutic agents: therapeutic applications. *Blood*. 2003;101:2377–2380.
22. Poulaki V, Mitsiades CS, Joussen AM, Lappas A, Kirchhof B, Mitsiades N. Constitutive nuclear factor-κB activity is crucial for human retinoblastoma cell viability. *Am J Pathol*. 2002;161: 2229–2240.
23. Mitsiades CS, Treon SP, Mitsiades N, et al. TRAIL/Apo2L ligand selectively induces apoptosis and overcomes drug resistance in multiple myeloma: therapeutic applications. *Blood*. 2001;98:795–804.
24. Pei XY, Dai Y, Grant S. The proteasome inhibitor bortezomib promotes mitochondrial injury and apoptosis induced by the small molecule Bcl-2 inhibitor HA14–1 in multiple myeloma cells. *Leukemia*. 2003;17:2036–2045.
25. Blaney SM, Bernstein M, Neville K, et al. Phase I study of the proteasome inhibitor bortezomib in pediatric patients with refractory solid tumors: a Children's Oncology Group study (ADVL0015). *J Clin Oncol*. 2004;22:4804–4809.
26. Horton TM, Pati D, Plon SE, et al. A phase 1 study of the proteasome inhibitor bortezomib in pediatric patients with refractory leukemia: a Children's Oncology Group study. *Clin Cancer Res*. 2007;13:1516–1522.
27. Giuliano M, Lauricella M, Calvaruso G, et al. The apoptotic effects and synergistic interaction of sodium butyrate and MG132 in human retinoblastoma Y79 cells. *Cancer Res*. 1999; 59:5586–5595.
28. Oda E, Ohki R, Murasawa H, et al. Noxa, a BH3-only member of the Bcl-2 family and candidate mediator of p53-induced apoptosis. *Science*. 2000;288:1053–1058.
29. Inbal B, Shani G, Cohen O, Kissil JL, Kimchi A. Death-associated protein kinase-related protein 1, a novel serine/threonine kinase involved in apoptosis. *Mol Cell Biol*. 2000;20:1044–1054.
30. Sanjo H, Kawai T, Akira S. DRAKs, novel serine/threonine kinases related to death-associated protein kinase that trigger apoptosis. *J Biol Chem*. 1998;273:29066–29071.
31. Rohde M, Daugaard M, Jensen MH, Helin K, Nylandsted J, Jaattela M. Members of the heat-shock protein 70 family promote cancer cell growth by distinct mechanisms. *Genes Dev*. 2005;19:570–582.
32. Sargent CA, Dunham I, Trowsdale J, Campbell RD. Human major histocompatibility complex contains genes for the major heat shock protein HSP70. *Proc Natl Acad Sci USA*. 1989;86:1968–1972.
33. Laroia G, Cuesta R, Brewer G, Schneider RJ. Control of mRNA decay by heat shock-ubiquitin-proteasome pathway. *Science*. 1999;284:499–502.
34. Doong H, Vrailas A, Kohn EC. What's in the 'BAG'?—a functional domain analysis of the BAG-family proteins. *Cancer Lett*. 2002;188: 25–32.
35. Sheikh MS, Hollander MC, Fornance AJ Jr. Role of Gadd45 in apoptosis. *Biochem Pharmacol*. 2000;59:43–45.
36. Friedman AD. GADD153/CHOP, a DNA damage-inducible protein, reduced CAAT/enhancer binding protein activities and increased apoptosis in 32D c13 myeloid cells. *Cancer Res*. 1996;56:3250–3256.
37. Guyton KZ, Xu Q, Holbrook NJ. Induction of the mammalian stress response gene GADD153 by oxidative stress: role of AP-1 element. *Biochem J*. 1996;314(pt 2):547–554.
38. Jin K, Mao XO, Eshoo MW, et al. cDNA microarray analysis of changes in gene expression induced by neuronal hypoxia in vitro. *Neurochem Res*. 2002;27:1105–1112.
39. Zimmermann J, Erdmann D, Lalande I, Grossenbacher R, Noorani M, Furst P. Proteasome inhibitor induced gene expression profiles reveal overexpression of transcriptional regulators ATF3, GADD153 and MAD1. *Oncogene*. 2000;19:2913–2920.
40. Oyadomari S, Mori M. Roles of CHOP/GADD153 in endoplasmic reticulum stress. *Cell Death Differ*. 2004;11:381–389.
41. Oyadomari S, Araki E, Mori M. Endoplasmic reticulum stress-mediated apoptosis in pancreatic beta-cells. *Apoptosis*. 2002;7:335–345.
42. Jiang HY, Wek SA, McGrath BC, et al. Activating transcription factor 3 is integral to the eukaryotic initiation factor 2 kinase stress response. *Mol Cell Biol*. 2004;24:1365–1377.
43. Zhang C, Gao C, Kawauchi J, Hashimoto Y, Tsuchida N, Kitajima S. Transcriptional activation of the human stress-inducible transcriptional repressor ATF3 gene promoter by p53. *Biochem Biophys Res Commun*. 2002;297:1302–1310.
44. Mashima T, Udagawa S, Tsuruo T. Involvement of transcriptional repressor ATF3 in acceleration of caspase protease activation during DNA damaging agent-induced apoptosis. *J Cell Physiol*. 2001; 188:352–358.
45. Zhang C, Kawauchi J, Adachi MT, et al. Activation of JNK and transcriptional repressor ATF3/LRF1 through the IRE1/TRAF2 pathway is implicated in human vascular endothelial cell death by homocysteine. *Biochem Biophys Res Commun*. 2001;289:718–724.
46. Hartman MG, Lu D, Kim ML, et al. Role for activating transcription factor 3 in stress-induced beta-cell apoptosis. *Mol Cell Biol*. 2004; 24:5721–5732.
47. Yan C, Jamaluddin MS, Aggarwal B, Myers J, Boyd DD. Gene expression profiling identifies activating transcription factor 3 as a

novel contributor to the proapoptotic effect of curcumin. *Mol Cancer Ther*. 2005;4:233–241.

48. Hollander MC, Zhan Q, Bae I, Fornace AJ Jr. Mammalian GADD34, an apoptosis- and DNA damage-inducible gene. *J Biol Chem*. 1997; 272:13731–13737.
49. Shah SA, Potter MW, McDade TP, et al. 26S proteasome inhibition induces apoptosis and limits growth of human pancreatic cancer. *J Cell Biochem*. 2001;82:110–122.
50. Poulaki V, Mitsiades CS, McMullan C, et al. Human retinoblastoma cells are resistant to apoptosis induced by death receptors: role of caspase-8 gene silencing. *Invest Ophthalmol Vis Sci*. 2005;46:358–366.
51. Lauricella M, Calvaruso G, Giuliano M, et al. Synergistic cytotoxic interactions between sodium butyrate, MG132 and camptothecin in human retinoblastoma Y79 cells. *Tumour Biol*. 2000;21:337–348.
52. Orlowski RZ, Voorhees PM, Garcia RA, et al. Phase 1 trial of the proteasome inhibitor bortezomib and pegylated liposomal doxorubicin in patients with advanced hematologic malignancies. *Blood*. 2005;105:3058–3065.